EXTENDED DATA

Targeting ferroptosis protects against multiorgan dysfunction and death.

Samya Van Coillie[1,2], Ines Goetschalckx[3], Bartosz Wiernicki[1,2], Banibrata Mukhopadhyay[4], Wulf Tonnus[5], Emily Van San[1,2], Sze Men Choi[1,2], Ria Roelandt[1,6], Catalina Dumitrascu[7], Ludwig Lamberts[3], Wannes Weyts[8], Jelle Huysentruyt[1,2], Behrouz Hassannia[1,2], Irina Ingold[9,10], Suhas Lele[4], Evelyne Meyer[11], Ruth Seurinck[1,6], Yvan Saeys[1,6], An Vermeulen[12], Alexander L.N. van Nuijs[7], Marcus Conrad[9,13], Andreas Linkermann[5,14], Mohan Rajapurkar[4], Peter Vandenabeele[1,2,15], Eric Hoste[16], Koen Augustyns[7] and Tom Vanden Berghe[1,2,3*].

[1]VIB-UGent Center for Inflammation Research; Ghent, Belgium.
[2]Department of Biomedical Molecular Biology; Ghent University, Ghent, Belgium.
[3]Department of Biomedical Sciences; University of Antwerp, Antwerp, Belgium.
[4]Department of Nephrology; Muljibhai Patel Society for Research in Nephro-Urology, Nadiad, India.
[5]Department of Internal Medicine 3, University Hospital Carl Gustav Carus; the Technische Universität Dresden, Dresden, Germany
[6]Department of Applied Mathematics, Computer Science and Statistics; Ghent University Ghent, Belgium
[7]Department of Pharmaceutical Sciences; University of Antwerp, Antwerp, Belgium.
[8]VIB-UGent Center for Medical Biotechnology; Ghent, Belgium.
[9]Institute of Metabolism and Cell Death, Helmholtz Zentrum München, German Research Center for Environmental Health; Munich, Germany
[10]Department of Medicine III, Klinikum rechts der Isar, Technical University of Munich, 81675 Munich, Germany
[11]Department of Pharmacology, Toxicology and Biochemistry, Ghent University; Merelbeke, Belgium
[12]Department of Bioanalysis; Ghent University, Ghent, Belgium.
[13]National Research Medical University, Laboratory of Experimental Oncology; Moscow, Russia
[14]Biotechnology Center; Technische Universität Dresden, 01307 Dresden, Germany
[15]Methusalem program; Ghent University, Ghent, Belgium.
[16]Department of Internal Medicine; Ghent University Hospital, Ghent, Belgium.

*Correspondence: T.V.B., Universiteitsplein 1, 2610 Antwerp, Belgium, T +3232659250, Tom.VandenBerghe@uantwerp.be.

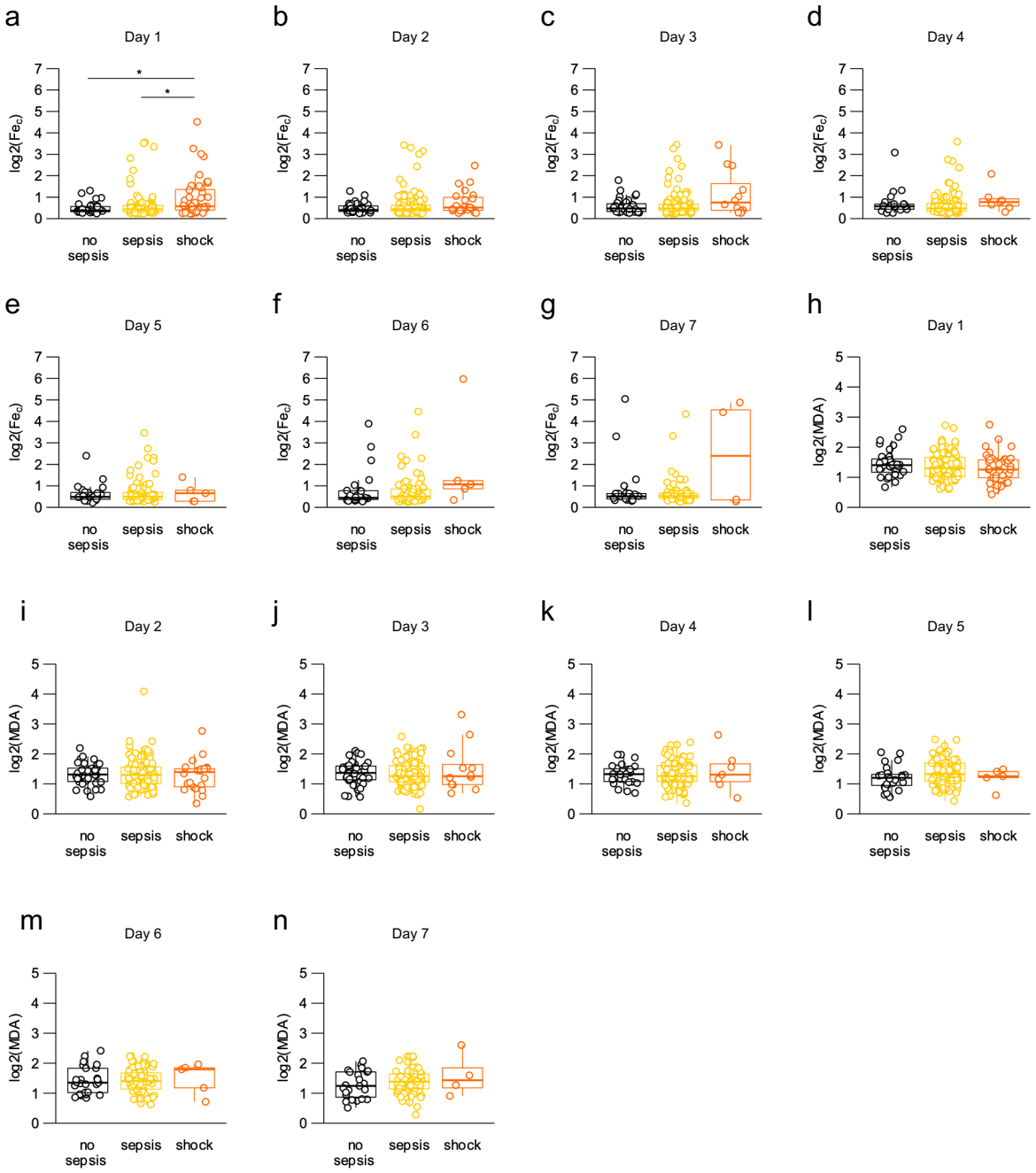

Extended data Fig. 1: Patients with sepsis cannot be distinguished from non-septic patients based on plasma catalytic iron (Fe_c) or MDA levels.

a-g, Boxplots showing the log-transformed catalytic iron (Fe_c) values from day 1 to 7 of all patients grouped by the presence of sepsis, septic shock or non-septic MODS. **h-n**, Boxplots showing the log-transformed malondialdehyde (MDA) values from day 1 to 7 of all patients grouped by the presence of sepsis, septic shock or non-septic MODS. **a-n**, Kruskal-Wallis (omnibus) and Wilcoxon-Mann-Whitney (pairwise) test. Error bars represent SEM; *P < 0.05.

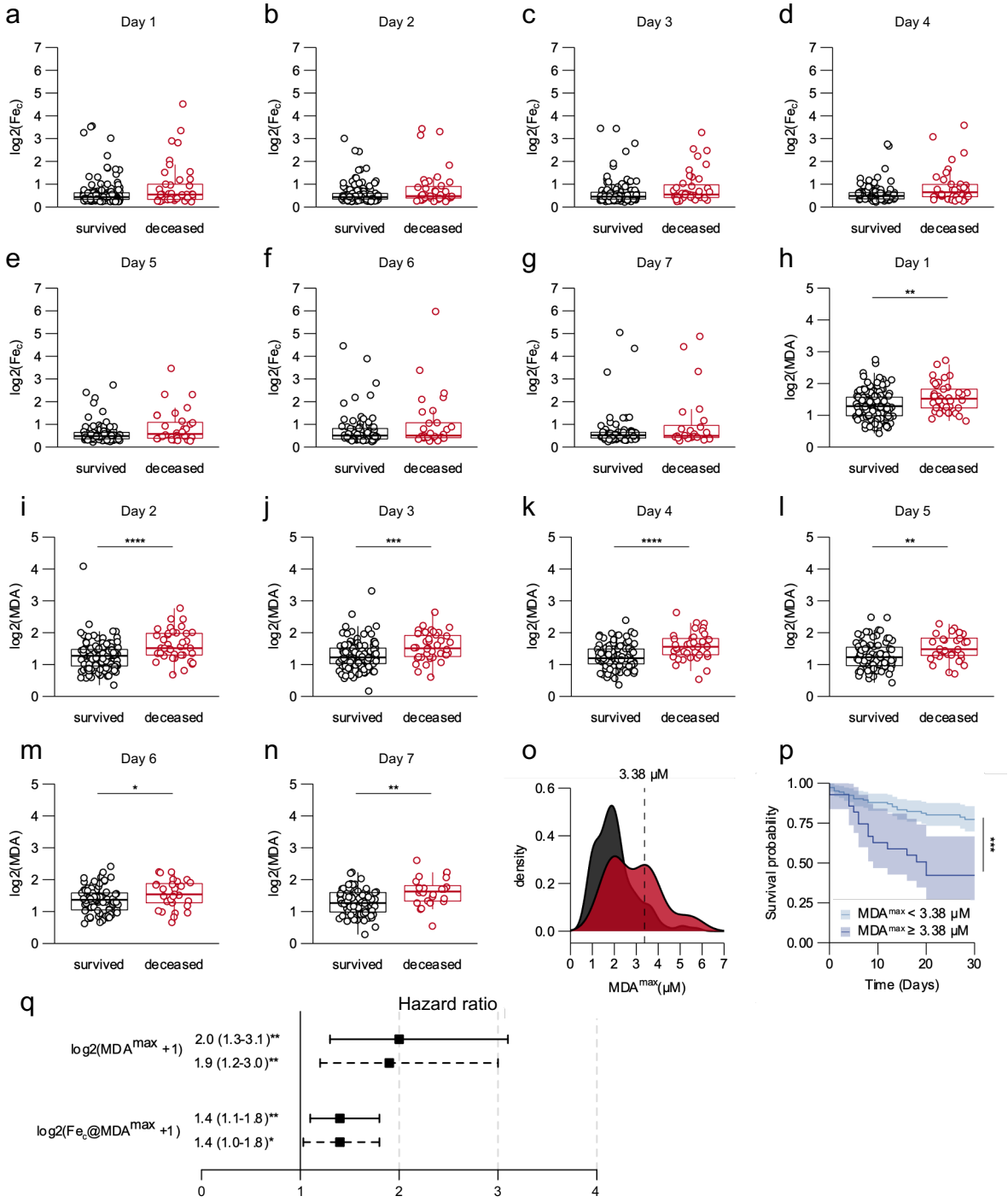

Extended data Fig. 2: MDA showed higher prognostic value for 30-day survival than catalytic iron.
a-g, Boxplots showing the log-transformed catalytic iron (Fe_c) values from day 1 to 7 of both the patients who passed away within 30 days and those who survived. **h-n**, Boxplots showing the log-transformed malondialdehyde (MDA) values from day 1 to 7 of both the patients who passed away within 30 days and those who survived. **o**, Histogram representing the density distribution of MDA^{max} values for both the patients who survive a 30-day survival follow-up (black) and those who do not (red). **p**, Survival curves representing the patients with values of MDA^{max} < 3.38 µM (light blue) and MDA^{max} ≥ 3.38 µM (dark blue). **q**, Forest plot summary representing the hazard ratio, $CI_{95\%}$ and associated p-value for the unadjusted predictors MDA^{max} level and corresponding Fe_c (full line) and for the predictors MDA^{max} level and corresponding Fe_c adjusted for age and SOFA score (dashed line) . **a-n**, Wilcoxon–Mann–Whitney test. **p**, Log-Rank test. **q**, Cox proportional hazards model. Error bars represent SEM; *P < 0.05, **P < 0.01, ***P < 0.001, ****P < 0.0001.

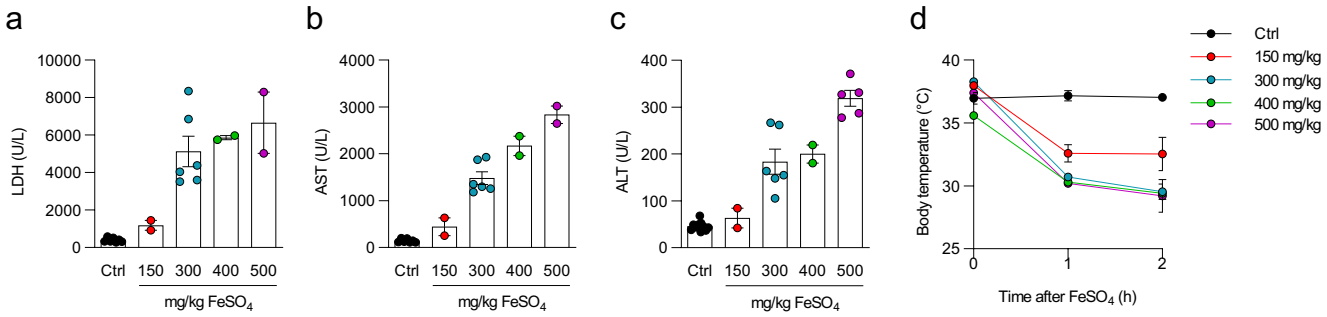

e

	FeSO4											
	ctrl		30'		2h		6h		12h			
	RTC	SEM	RTC	SEM	RTC	SEM	RTC	SEM	RTC	SEM	N	n
Ileum	1.0	0.2	8.4	2.3	8.2	2.3	8.7	2.5	11.9	3.3	3	6
Liver	1.0	0.0	2.1	0.2	2.3	0.2	2.9	0.2	3.4	0.2	3	6
Kidney	1.0	0.0	1.9	0.1	1.8	0.1	1.6	0.1	2.0	0.3	3	6
Spleen	1.0	0.0	1.3	0.2	1.2	0.1	1.2	0.2	2.1	0.2	3	6
Brain	1.0	0.0	1.1	0.1	1.2	0.2	1.4	0.2	1.4	0.1	3	6
Lung	1.0	0.1	1.2	0.1	1.1	0.1	1.1	0.1	1.5	0.3	3	6
Muscle	1.0	0.1	0.7	0.2	1.0	0.2	0.8	0.2	0.9	0.3	3	6
Heart	1.0	0.1	0.9	0.1	1.0	0.1	0.9	0.1	1.1	0.1	3	6
Plasma	1.0	0.1	7.7	1.3	4.3	0.2	2.1	0.2	2.0	0.1	3	5-6

Relative iron level

f

	FeSO4															
	ctrl		30'		1h		2h		4h		6h		12h			
	RTC	SEM	RTC	SEM	RTC	SEM	RTC	SEM	RTC	SEM	RTC	SEM	RTC	SEM	N	n
CK	1.0	0.1	7.5	1.8	9.8	1.2	16.3	3.3	30.5	4.6	66.4	11.9	84.3	7.6	5	6-10
LDH	1.0	0.0	2.6	0.5	3.9	0.4	5.9	1.3	12.5	1.8	30.6	5.6	58.7	10.0	5	6-10
AST	1.0	0.1	3.8	0.7	5.2	0.4	6.8	0.8	9.7	1.1	10.8	1.1	13.1	1.3	5	6-10
ALT	1.0	0.0	1.7	0.2	2.1	0.1	2.8	0.3	4.7	0.8	4.0	0.3	7.0	1.4	5	6-9
Trop T	1.0	0.1	2.5	1.1	2.3	0.3	1.8	0.2	2.6	0.2	3.3	0.2	4.9	1.2	6	6-8
Cr	1.0	0.0	1.2	0.1	1.0	0.0	2.5	0.2	2.4	0.3	2.5	0.5	1.8	0.4	6	8-13
Urea	1.0	0.0	1.3	0.0	1.4	0.1	1.8	0.0	2.0	0.2	2.4	0.2	2.2	0.3	4	6-9
Mb	1.0	0.1	1.4	0.1	1.2	0.1	1.8	0.4	1.3	0.2	1.2	0.1	1.0	0.2	4	6-10
Ferritin	1.0	0.0	1.0	0.0	1.3	0.1	1.1	0.0	1.4	0.1	1.4	0.1	1.5	0.1	3	6-7

Relative level in plasma

g

	FeSO4															
	ctrl		30'		1h		2h		4h		6h		12h			
	RTC	SEM	RTC	SEM	RTC	SEM	RTC	SEM	RTC	SEM	RTC	SEM	RTC	SEM	N	n
Kidney	1.0	0.1	4.2	0.5	4.4	0.8	4.0	0.7	4.4	0.6	3.0	0.4	3.1	0.5	3	5-6
Liver	1.0	0.0	3.6	1.1	3.4	1.0	3.3	0.6	3.4	1.3	2.9	0.9	3.2	1.5	3	5-6
Ileum	1.0	0.1	2.3	0.3	1.4	0.2	1.7	0.3	1.5	0.2	1.4	0.1	1.5	0.2	3	5-8
Muscle	1.0	0.1	1.4	0.2	1.1	0.2	1.1	0.2	1.4	0.2	1.1	0.1	1.2	0.3	3	6-8
Spleen	1.0	0.0	1.2	0.2	1.0	0.3	0.8	0.1	1.5	0.4	1.3	0.2	1.2	0.3	3	5-6
Heart	1.0	0.2	1.0	0.1	0.7	0.1	0.8	0.0	1.0	0.2	1.4	0.2	1.3	0.1	3	5-6
Brain	1.0	0.1	1.0	0.0	1.2	0.2	1.0	0.1	1.0	0.1	1.0	0.1	0.9	0.1	3	5-8
Lung	1.0	0.1	0.9	0.1	0.6	0.1	0.6	0.1	0.7	0.1	0.6	0.1	0.6	0.1	3	5-6
Plasma	1.0	0.1	1.8	0.2	1.7	0.2	1.6	0.2	1.4	0.1	1.6	0.3	1.0	0.1	3	5-8

Relative MDA level

Extended data Fig. 3: Dose optimization and characterization of iron sulphate as iron overload model. **a-c**, Plasma levels of LDH, AST and ALT 2h after injection of different dosages of iron sulphate ranging from 150 to 500 mg/kg (n = 2-6/condition). **d**, Body temperature 2h after injection of different dosages of iron sulphate ranging from 150 to 500 mg/kg (n = 2-6/condition). **e-g**, Tables representing the relative iron levels, plasma damage markers and MDA levels after acute iron overload as a function of time. N represents the number of independently performed experiments; n represents the total number of mice per time point. RTC, relative to control; SEM, standard error of the mean.

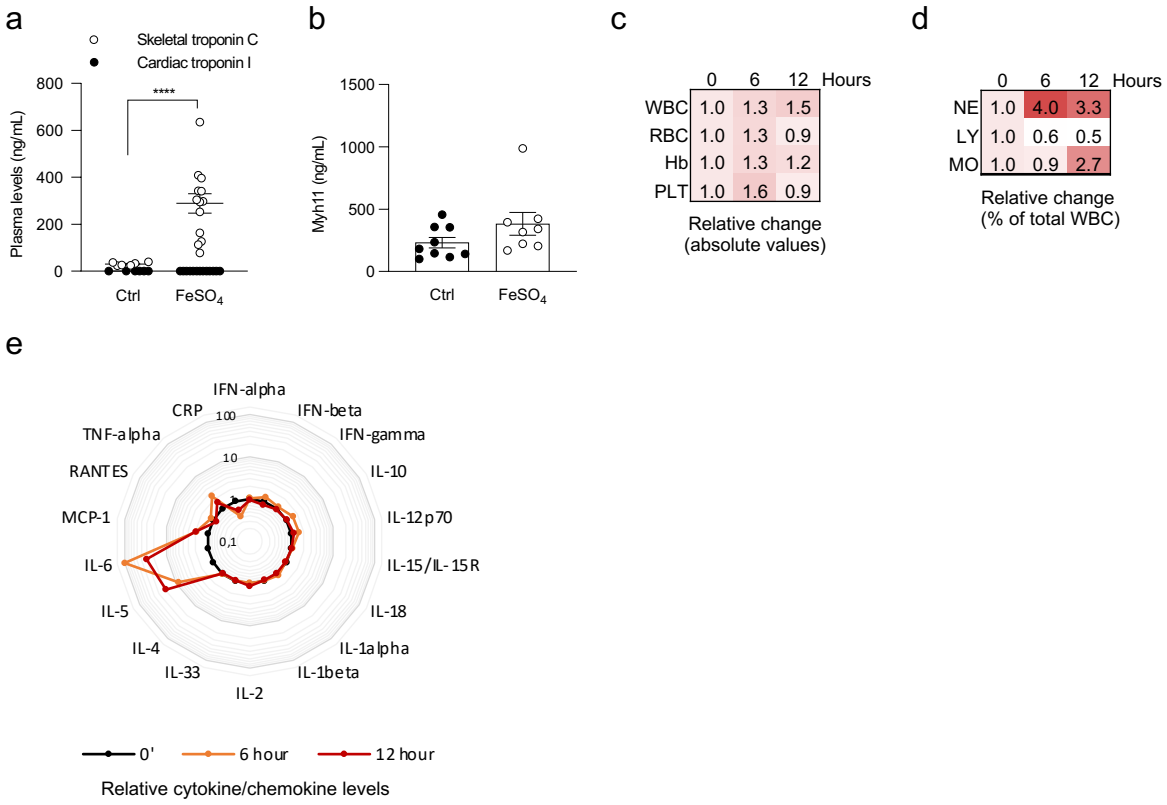

Extended data Fig. 4: Acute iron overload causes skeletal muscle injury, neutrophilia, lymphopenia and elevated levels of plasma IL-6 and -5.

a, Plasma levels of skeletal troponin C and cardiac troponin I 2h after iron overload. The combined results of 2 independent experiments are shown (total n = 6-13/condition). **b**, Plasma levels of Myosin heavy chain 11 (Myh11) 2h after iron overload, reflecting smooth muscle injury. The combined results of minimum 2 independent experiments are shown (total n = 8-9/condition). **c**, Heatmap representing the relative blood count after iron overload as a function of time. The combined results of 3 independent experiments are shown (total n = 6-7/timepoint). **d**, Heatmap representing the relative change in WBC populations after iron overload as a function of time in plasma. The combined results of 3 independent experiments are shown (total n = 6-7/timepoint).**e**, Radar web representing the relative cytokine and chemokine levels after iron overload as a function of time. The combined results of 3 independent experiments are shown (total n = 5-6/timepoint). **a**, Pairwise T statistics. Error bars represent SEM; ****P < 0.0001.

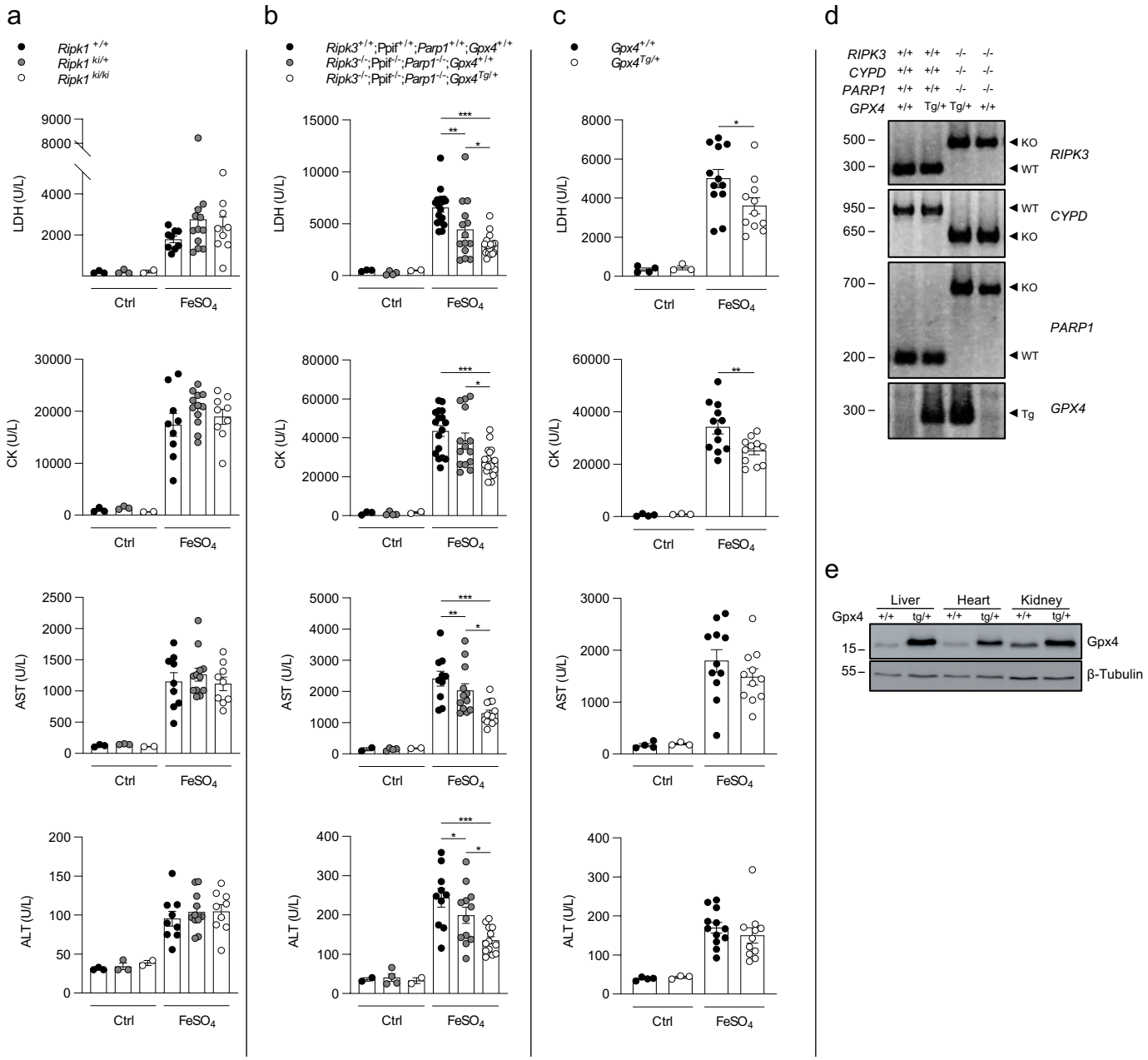

Extended data Fig. 5: RIPK1, RIPK3, CypD and PARP1 are not critically involved in iron overload induced injury.

a, Plasma levels of LDH, CK, AST and ALT 2h after iron overload for RIPK1 kinase dead mice (*Ripk1*$^{ki/ki}$). The combined results of minimum 2 independent experiments are shown (total n = 2-12/condition). **b**, Plasma levels of LDH, CK, AST and ALT 2h after iron overload for mice triple-deficient in RIPK3, CypD and PARP1 (*Ripk3*$^{-/-}$;*Ppif*$^{-/-}$;*Parp*$^{-/-}$). The combined results of minimum 2 independent experiments are shown (total n = 2-18/condition). **c**, Plasma levels of LDH, CK, AST and ALT 2h after iron overload for GPX4 overexpressing mice (*Gpx4*$^{Tg/+}$). The combined results of minimum 2 independent experiments are shown (total n = 3-12). **d**, PCR reaction illustrating the deficiency of Ripk3, Ppif and Parp1 with or without transgenic expression of Gpx4 in the *Ripk3*$^{-/-}$;*Ppif*$^{-/-}$;*Parp*$^{-/-}$*Gpx4*$^{Tg/+}$ mouse line. **e**, Western blot illustrating the overexpression of GPX4 in liver, heart and kidney tissue of *Gpx4*$^{Tg/+}$ mice. These experiments were performed on synthetic diet containing 50 mg/kg vitamin E. **a**,**b**, pairwise comparisons via the Fisher's unprotected LSD test. **c**, pairwise T statistics. Error bars represent SEM; *P < 0.05, **P < 0.01, ***P < 0.001.

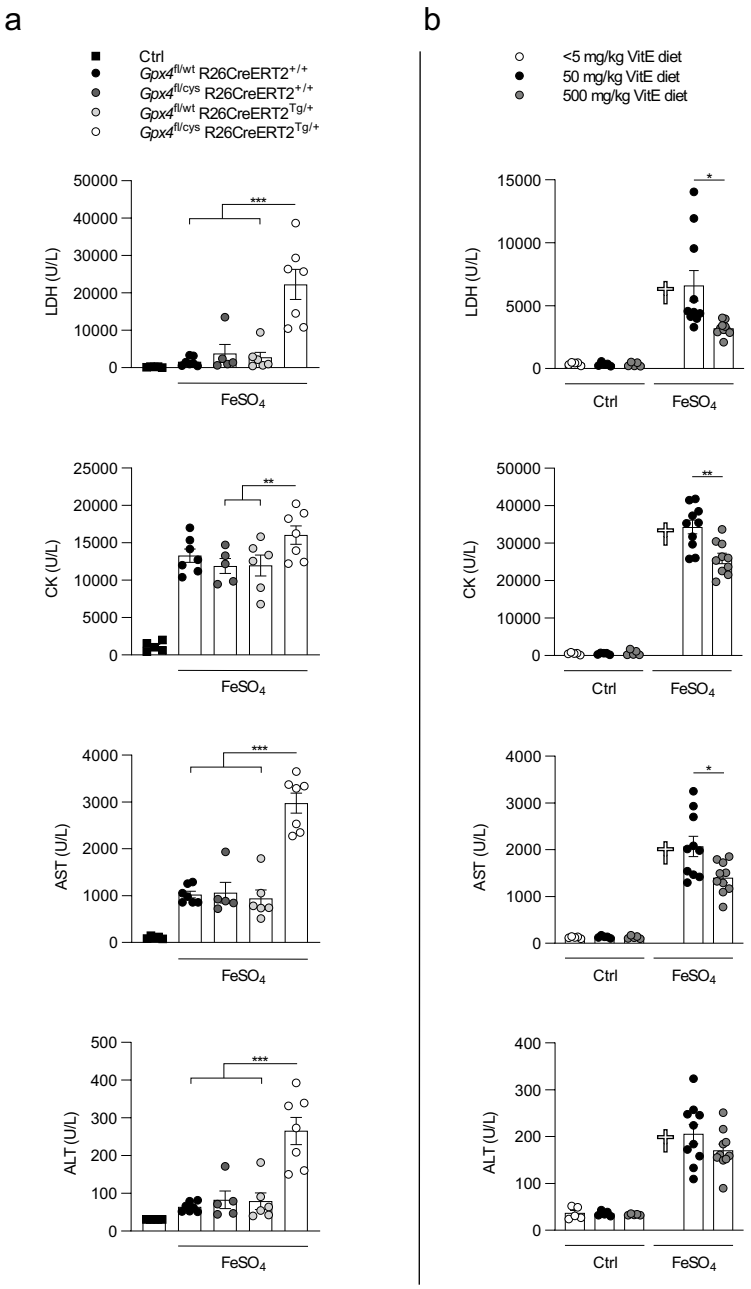

Extended data Fig. 6: Iron overload induced injury is reduced by a vitamin E-rich diet, while ferroptosis sentinel mice expressing the cysteine mutant of GPX4 show highly exacerbated injury.

a, Plasma levels of LDH, CK, AST and ALT 2h after iron overload for mice expressing the GPX4 cysteine mutant. The combined results of minimum 2 independent experiments are shown (total n = 5-7).

b, Plasma levels of LDH, CK, AST and ALT 2h after iron overload for mice receiving different dietary levels of vitamin E (<5/50/500 mg/kg). The combined results of 2 independent experiments are shown (total n = 5-10). The cross symbol represents death of the mice. **a**, pairwise comparisons via the Fisher's unprotected LSD test. **b**, pairwise T statistics. Error bars represent SEM. *P < 0.05, **P < 0.01, ***P < 0.001.

a

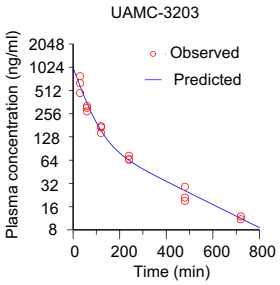

b

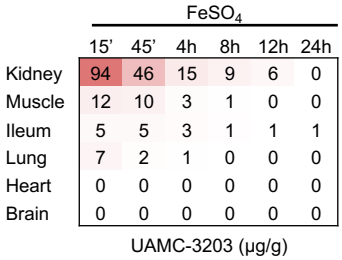

c

Table 1 In vivo PK analysis of UAMC-3203 in mice

	C_0 (µg/mL or µg/g)	k_e (1/hr)	$t_{1/2}$ (hr)	$AUC_{0\text{-inf}}$ (µg*hr/mL or µg*hr/g)	T/P	$A_{av.ss}$ (ng)
Plasma	1.01	0.214	3.24	1.34	-	1.92
Intestine	5.58	0.176	3.94	40.2	30.0	85.2
Kidney	133	0.242	2.86	294	219	3197
Lung	6.00	0.232	2.99	14.0	10.5	78.8
Muscle*	13.0	0.359	1.93	39.8	29.7	215

* $t_{1/2}$ calculated using mean values

Both for intestine and muscle. the time point at 24h was excluded for the calculation of $t_{1/2}$

d

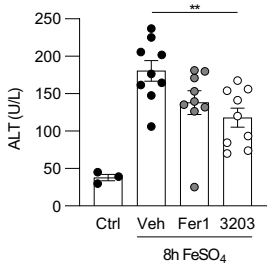

e

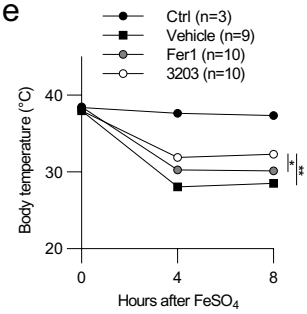

f

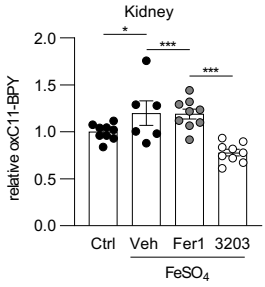

Extended data Fig. 7: *In vivo* plasma and tissue PK properties of UAMC-3203, which reduces organ injury, lipid peroxidation, and the drop of body temperature after iron overload.

a, Plasma concentrations of UAMC-3203 as a function of time (total n = 3/time point) in mice after intravenous bolus dosing at 12.35 mg/kg. **b**, Concentrations of UAMC-3203 as a function of time in kidney, muscle, ileum, lung, heart and brain tissue (total n = 3/time point) of mice after intravenous bolus dosing at 12.35 mg/kg. **c**, Table showing the concentration of UAMC-3203 at time 0 (C_0), its elimination rate constant (k_e), its elimination half-life ($t_{1/2}$), its total area under the curve ($AUC_{0\text{-inf}}$), its tissue to plasma ratio (T/P) and its average amount in tissue at steady-state ($A_{av,ss}$) in plasma, intestine, kidney, lung and muscle tissue (total n = 3/time point) in mice after intravenous bolus dosing at 12.35 mg/kg. **d**, Plasma levels of ALT 8h after iron overload for mice treated with vehicle (2% DMSO), Fer1, or compound UAMC-3203. The combined results of minimum 2 independent experiments are shown (total n = 3-9/condition). **e**, Body temperature 8h after iron overload for mice treated with vehicle (2% DMSO), Fer1 or compound UAMC-3203. The combined results of minimum 2 independent experiments are shown (total n = 3-10/condition). **f**, Relative measure of lipid peroxidation in kidney tissue detected by flow cytometry in the form of oxidized C11-BODIPY staining 30 min after iron overload for mice treated with vehicle (2% DMSO), Fer1 or compound UAMC-3203. The combined results of 3 independent experiments are shown (total n = 6-9/condition). **d**,**f**, pairwise comparisons via Fisher's unprotected LSD test. **e**, method of residual maximum likelihood (REML) with approximate *F*-test. Error bars represent SEM. *P < 0.05, **P < 0.01, ***P < 0.001.

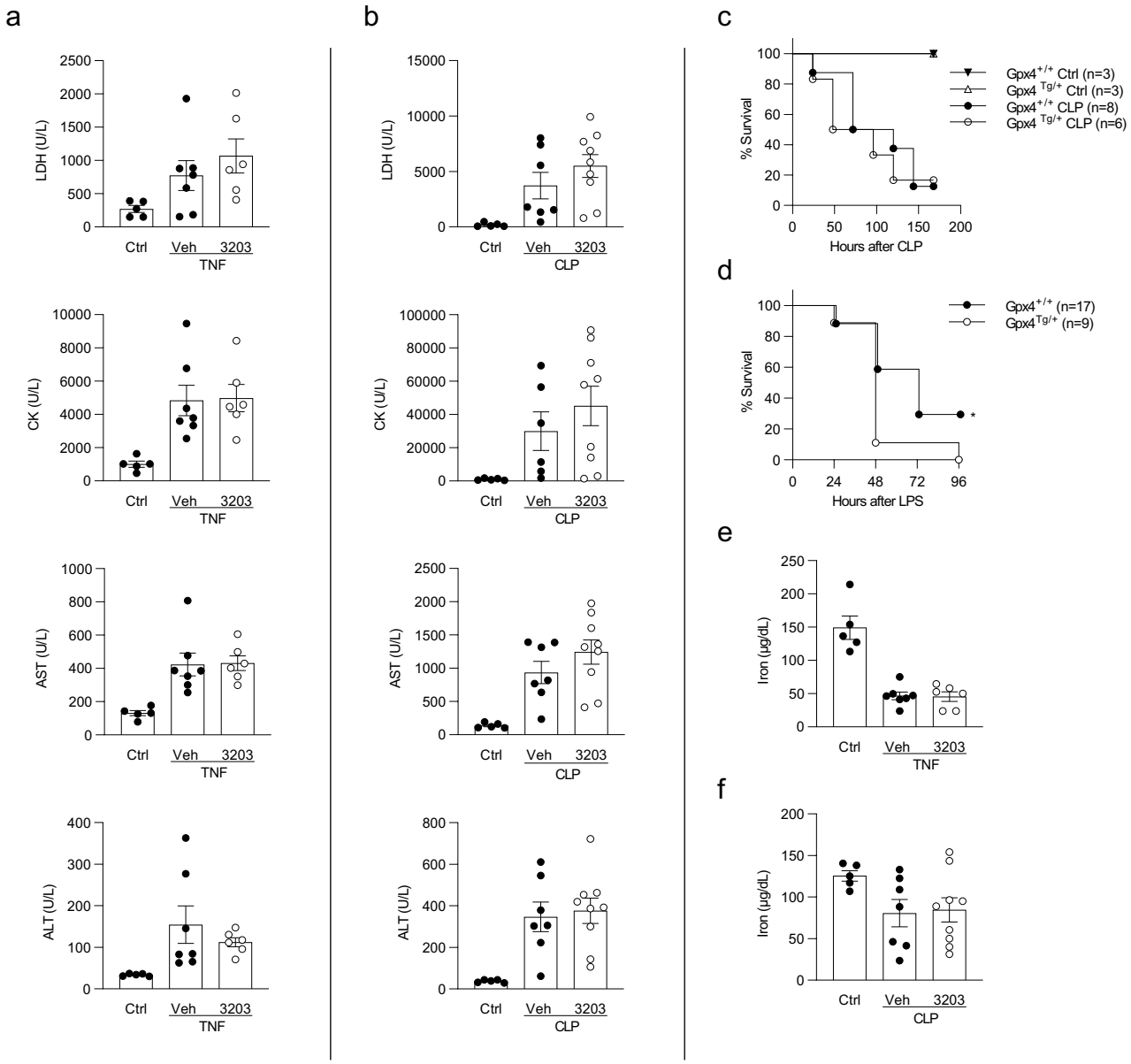

Extended data Fig. 8: Blocking ferroptosis is not effective as treatment for sepsis and septic shock.
a, Plasma levels of LDH, CK, AST and ALT 8h after TNF challenge for mice treated with vehicle (2% DMSO) or compound UAMC-3203. The combined results of 2 independent experiments are shown (total n = 5-7/condition). **b**, Plasma levels of LDH, CK, AST and ALT 24h after CLP for mice treated with vehicle (2% DMSO) or compound UAMC-3203. The combined results of 2 independent experiments are shown (total n = 5-9/condition). **c**, Survival curve of $Gpx_4^{Tg/+}$ mice after CLP. The combined results of 2 independent experiments are shown (total n = 3-8/condition). **d**, Survival curve of $Gpx_4^{Tg/+}$ mice after LPS challenge. The combined results of minimum 3 independent experiments are shown (total n = 9-17/condition). **e**, Plasma iron levels 8h after TNF challenge for mice treated with vehicle (2% DMSO) or compound UAMC-3203. The combined results of 2 independent experiments are shown (total n = 5-7/condition). **f**, Plasma iron levels 24h after CLP for mice treated with vehicle (2% DMSO) or compound UAMC-3203. The combined results of 2 independent experiments are shown (total n = 5-9/condition). The TNF experiments were performed on mice with a C57BL6/J background. **a**,**b**,**e**,**f**, pairwise T statistics. **c**,**d**, Mantel-Cox test. Error bars represent SEM. *P < 0.05.

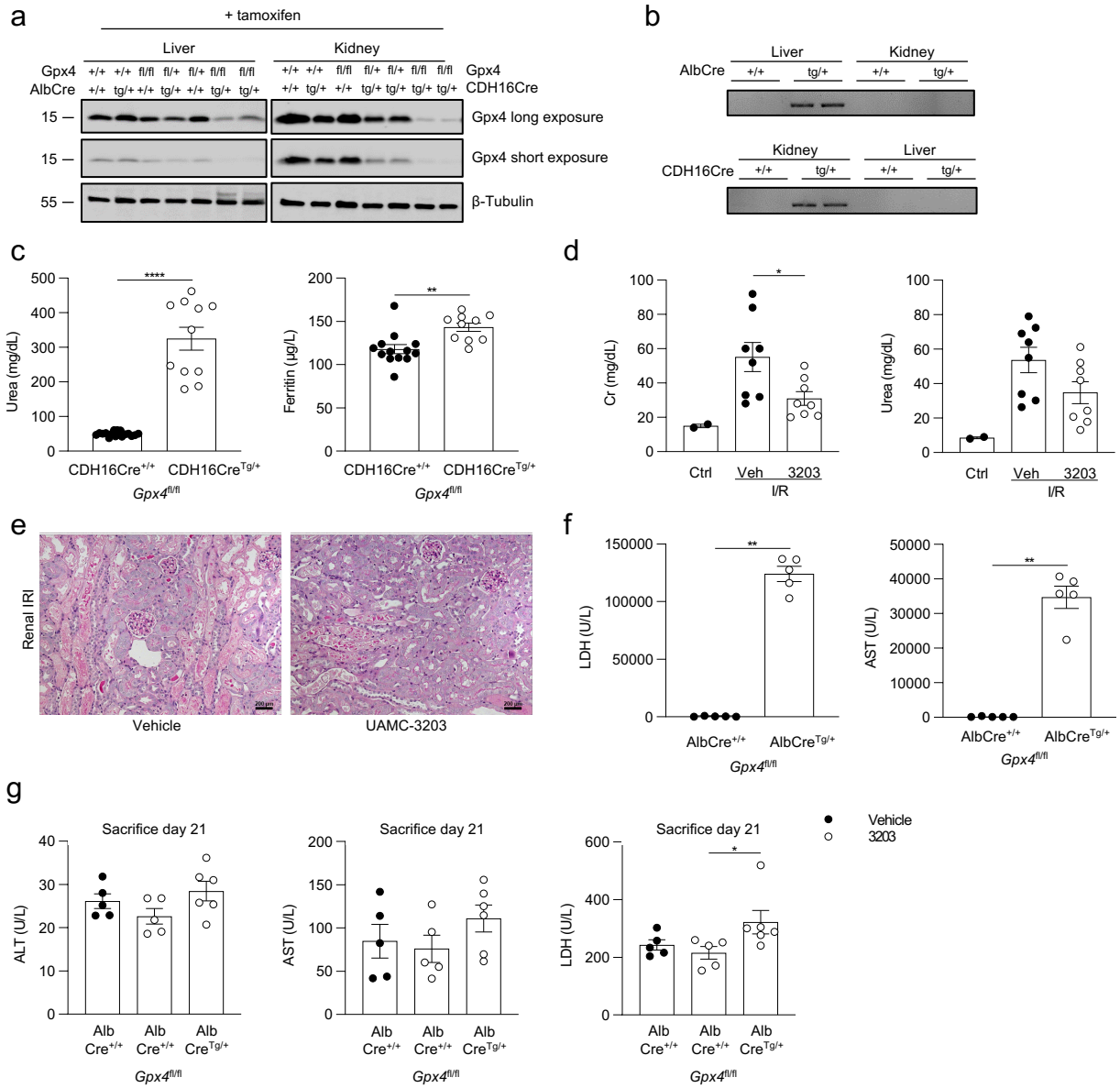

Extended data Fig. 9: Genetic models of ferroptosis driven acute liver and kidney injury.
a, Western blot illustrating the knock down of GPX4 in liver tissue of *Gpx4*$^{fl/fl}$ AlbCreERT2$^{Tg/+}$ and in kidney tissue of *Gpx4*$^{fl/fl}$ CDH16CreERT2$^{Tg/+}$ mice upon TAM administration. **b**, PCR gel with primers binding only upon excision of *Gpx4* performed on liver (vs kidney) tissue of *Gpx4*$^{fl/fl}$ AlbCreERT2$^{Tg/+}$ mice and kidney (vs liver) tissue of *Gpx4*$^{fl/fl}$ CDH16CreERT2$^{Tg/+}$ mice upon TAM administration. **c**, Plasma levels of urea and ferritin of *Gpx4*$^{fl/fl}$ CDH16CreERT2$^{Tg/+}$ mice which were sacrificed 6 days after TAM administration. The combined results of 2 independent experiments are shown (total n = 10-13/condition). **d**, Plasma levels of Cr and urea 48h after ischemia reperfusion for mice treated with vehicle (2% DMSO) or compound UAMC-3203 (total n = 2-8/condition). This experiment was performed with C57Bl/6N mice provided by Charles River. **e**, Histological PAS staining of kidney tissue 48h after ischemia reperfusion for mice treated with vehicle (2% DMSO) or compound UAMC-3203 (total n = 2-8/condition). This experiment was performed with C57Bl/6N mice provided by Charles River. **f**, Plasma levels of LDH and AST of *Gpx4*$^{fl/fl}$ AlbCreERT2$^{Tg/+}$ mice which were sacrificed once a human endpoint was reached. The combined results of 2 independent experiments are shown (total n = 5/condition). **g**, Plasma levels of ALT, AST and LDH of *Gpx4*$^{fl/fl}$ AlbCreERT2$^{Tg/+}$ mice sacrificed on day 21 (16 days after final TAM administration) which were treated daily with vehicle (2% DMSO) or compound UAMC-3203. The combined results of 4 independent experiments are shown (total n = 5-6/condition). **c**,**d**,**f**,**g**, pairwise T statistics. Error bars represent SEM. *P < 0.05, **P < 0.01, ****P < 0.0001.